

The Role of Interface Domain Interactions on Thermal Stability of DNA polymerase I ITB-1

Santi Nurbaiti¹, Rukman Hertadi¹, Muhamad A. Martoprawiro² and Akhmaloka^{*,1}

¹Biochemistry Research Division, Faculty of Mathematics and Natural Science, Institut Teknologi Bandung, Jln Ganesha 10, Bandung 40132, Indonesia

²Inorganic and Physical Chemistry Research Division, Faculty of Mathematics and Natural Science, Institut Teknologi Bandung, Jln Ganesha 10, Bandung 40132, Indonesia

Abstract: Temperature-induced unfolding of Klenow-like DNA Pol I ITB-1 was investigated by molecular dynamic simulation, focusing on the key factors that stabilizing the protein. The result showed that the protein unfolded initially by disruptions of the interface between of 5'→3' polymerase and 3'→5' exonuclease domains. Several amino acid residues, Lys374-Glu489 and Lys381-Glu487, form salt bridges at the interface domain and played an important role in the contact between the two domains. These interactions were examined through *in silico* mutation by comparing the free-energy solvation changes between the wild type and the mutants. The disruption of salt bridges by replacing Glu to Gln at position 487 and 489 caused positive value of $\Delta\Delta G_{\text{sol}}$, suggesting that the proteins were more unstable. While the substitution of Glu to Asp at position 487 and 489 preserved the electrostatic interaction. The last two mutants showed negative value of $\Delta\Delta G_{\text{sol}}$, suggesting that the proteins were more stable. All the data suggested that the salt bridges between Lys374-Glu489 and Lys381-Glu487 have an essential role in maintaining the stability of the interface domain of DNA Pol I ITB-1, and thus, the whole structure of the protein.

Keywords: DNA polymerase I ITB-1, molecular dynamic simulation, salt bridges, free-energy calculation.

INTRODUCTION

DNA polymerases are molecular motors that direct the synthesis of DNA from mono nucleotides. Based on the sequence similarity and crystal structure, polymerases are classified into seven different families: A, B, C, D, X, Y, and RT families [1-4]. The most extensively studied DNA polymerases are from A family. The *Escherichia coli* DNA Pol I and *Thermus aquaticus* (*Taq*) DNA Pol I are the most characterized DNA Pol from A family [5, 6]. The structure of all known polymerases showed that these enzymes contain three subdomains that are associated with the binding of DNA primer-template and an incoming dNTP, termed as palm, fingers, and thumb. The palm is the most conserved region, contained two carboxylate residues that had important role on phosphoryl transfer reaction [7].

DNA polymerases have been used extensively in molecular biological research, especially in PCR and sequencing techniques. Thermostable DNA polymerases, such as *Taq* DNA Pol I, have been the key element in the development of the polymerase chain reaction [8, 9], since the enzyme is still stable at high temperature up to 97°C. Several high thermostable DNA polymerases have been studied from different organisms [10-14]. A few moderate thermostable DNA polymerases have been isolated and

purified from thermophilic *Bacillus* species [15, 16]. *Bst* DNA polymerase was isolated from *B. stearothermophilus* [17-19]. *Bca* DNA polymerase was isolated and cloned from *B. caldotenax* [19, 20]. *Bst* DNA polymerase has been used for DNA sequencing. All the above enzymes showed less optimal temperature for polymerase reaction. However, the amino acid sequences of the enzymes are not significantly different with the high thermostable DNA polymerases.

Understanding the mechanism of thermal stability of protein has been the subject of exhaustive experimental and theoretical studies for more than few decades. The experimental approaches carried out by comparison of the amino acids sequences or crystal structures showed no general rule for the factors involved in thermal stability of proteins [21]. Thermal stability depends on the combination of many factors [22-25]. The use of molecular dynamic (MD) simulation over the last 20 years provided the ultimate detail concerning individual atomic motion and become a standard tool for the investigation of biomolecules [26]. Understanding of motion behavior at the atomic level is a valuable factor for the study of complicated reactions, such as folding or unfolding protein. In addition, the motion behavior is also important for exploring the conformational space, such as ligand-docking or investigating natural dynamics of protein at elevated temperature, which is not easily obtained by experimental analysis [26-30]. This theoretical approach has been used to elucidate factors that govern thermostability of proteins at atomic level [31-33]. Furthermore, complementation between the experimental and the computational analysis provides more complete and detailed pictures of the biomolecules.

*Address correspondence to this author at the Biochemistry Research Division, Faculty of Mathematics and Natural Science, Institut Teknologi Bandung, Jln Ganesha 10, Bandung 40132, Indonesia; Tel: (62)22-2502103; Fax: (62)22-2504154; E-mail: loka@chem.itb.ac.id

A moderate thermostable DNA polymerase from *Geobacillus thermoleovorans* has been cloned and expressed in *E. coli*, namely DNA polymerase I (Pol I) ITB-1. This enzyme consists of three structural domains, 5'→3' polymerase, 3'→5' exonuclease and 5'→3' exonuclease domains. The enzyme has optimal polymerase temperature 338K (65°C) [34]. Initial effort to understand the molecular basis for thermal stability of the enzyme was carried out by molecular dynamic simulations at 400K and 500K [35]. The result showed that the β -sheets 2, 3 and 4 [36] in the 3'→5' exonuclease domain were the most thermo-labile segment of the enzyme. However, prediction of detailed molecular interactions, which was responsible for the thermal stability, was hard to obtain, due to the spontaneous unfolding of the enzyme at these temperatures. Hence, in this report we would like to present the factors that are involved in thermal stability of DNA Pol I ITB-1 using molecular dynamic simulation at lower temperature.

METHODS

Construction of Structural Model

The initial three-dimensional structure of DNA Pol I ITB-1 was constructed on the basis of homological protein structure modeling from SwissProt using *Predict Protein* program [37]. Three steps for using the comparative modeling program, alignment of amino acids sequences, structure prediction, and validation of structure using WHAT_IF SwissProt Program, were carried out to construct the protein model.

Simulation Method

Amber version 9.0 program [38] was used for the molecular dynamic simulation. To improve simulation efficiency, only those bond lengths that involved hydrogen atoms were constrained with the SHAKE algorithm [39]. Parm99 + frcmod ff03 [40] was used for the simulation. The implicit solvent (igb =5) was used to describe the solvation effects in MD simulations. The mbondi2 radii were set, and the reaction field cutoff (rgbmax = 16) was employed to speed-up the calculation of effective Born radii. The salt concentration was set at 0.5 M during the whole simulation. The structure was subjected to energy minimization calculations by the steepest descent method with 500 iterations, followed by the conjugate gradient method with 4500 iterations to be used as starting lowest energy structure. The energy-minimized state of protein was then submitted to MD simulations after equilibrating for about 100 ps at 300K and 350K, respectively. The temperature and pressure were kept constant, during the simulation by coupling the system to Berendsen heat bath at the simulation temperature and an external pressure bath at 1 atm, with a relaxation time of 4 ps, respectively. The trajectories and coordinates of the proteins were saved every 2 fs for structural analysis. Simulation image of protein was generated by visual molecular dynamics (VMD) software [41].

Free Energy Calculation

The overall free energy perturbation (FEP) was calculated by using the alchemical free energy simulation

module in NAMD 2.6 [42]. All simulations were carried out with periodic boundary condition (100×100×100 Å³ periodic box) at constant temperature (350K) and pressure of 1 bar, using PME electrostatics. Ten Langevin dynamics simulations were performed with $\delta\lambda$ that was 0.1. The FEP calculations were run until the λ get to the value 1.0, and in every λ , 50000MD step were carried out. The trajectories were saved every 2 fs. Solvation in explicit water was built, using solvate plugin on VMD. A topology file containing hybrid amino acids for all point mutations was constructed with the VMD plugin Mutator, based on the standard CHARMM topologies. The solvated system was equilibrated at the target temperature and pressure then run to FEP simulation in the NPT ensemble.

Analysis of MD Trajectories

Analysis of the MD coordinate trajectories of the simulations was performed by calculating several structural parameter over time, such as C- α root-mean-square deviations (RMSD), root-mean-square fluctuation (RMSF), solvent accessible surface area (SASA), and percentage of secondary structure (% SS). RMSDs and RMSFs were calculated within the software package VMD. The RMSDs were calculated for the backbone atoms with reference to the starting structure at $t = 0$. This could be expressed in the following equation:

$$RMSD = \sqrt{\frac{\sum_{i=1}^{N_{atoms}} (r_i(t_1) - r_i(t_2))^2}{N_{atoms}}} \quad (1)$$

where, N is the total number of atoms, while $r_i(t_2)$ and $r_i(t_1)$ represent the coordinates of atom i at time t and at initial stage (t_1), respectively.

The atomic fluctuation in the protein was studied by computing the RMSFs of the structures generated from the simulation.

$$RMSF = \sqrt{\left[R_j - |R_j| \right]^2} \quad (2)$$

where, R_j is the coordinate of residues j , and $|R_j|$ represents the average of the j atom. SASA and % SS were calculated by using Dictionary of Protein Secondary Structure (DSSP) software [43].

RESULTS

Structure of DNA Pol I ITB-1

Three dimensional structure of Klenow-like DNA Pol I ITB-1 was modeled by homological protein structure modeling from SwissProt, using *Predict Protein* program [37]. A fragment of DNA Pol I ITB-1 from residue 297 to 876, containing 5'→3' polymerase and 3'→5' exonuclease regions, was selected for the construction of the 3D structure of the enzyme. The crystal structure of *Bacillus* fragment (BF) DNA Pol I from *B. stearothermophilus* (PDB entry 1XWL [44]) was chosen as a template for the comparative modeling, since the amino acids sequence for the region has identity more than 95% compared to that DNA Pol I ITB-1. The 3D structure of DNA Pol I ITB-1, generated from the comparative modeling, almost resembled with the crystal

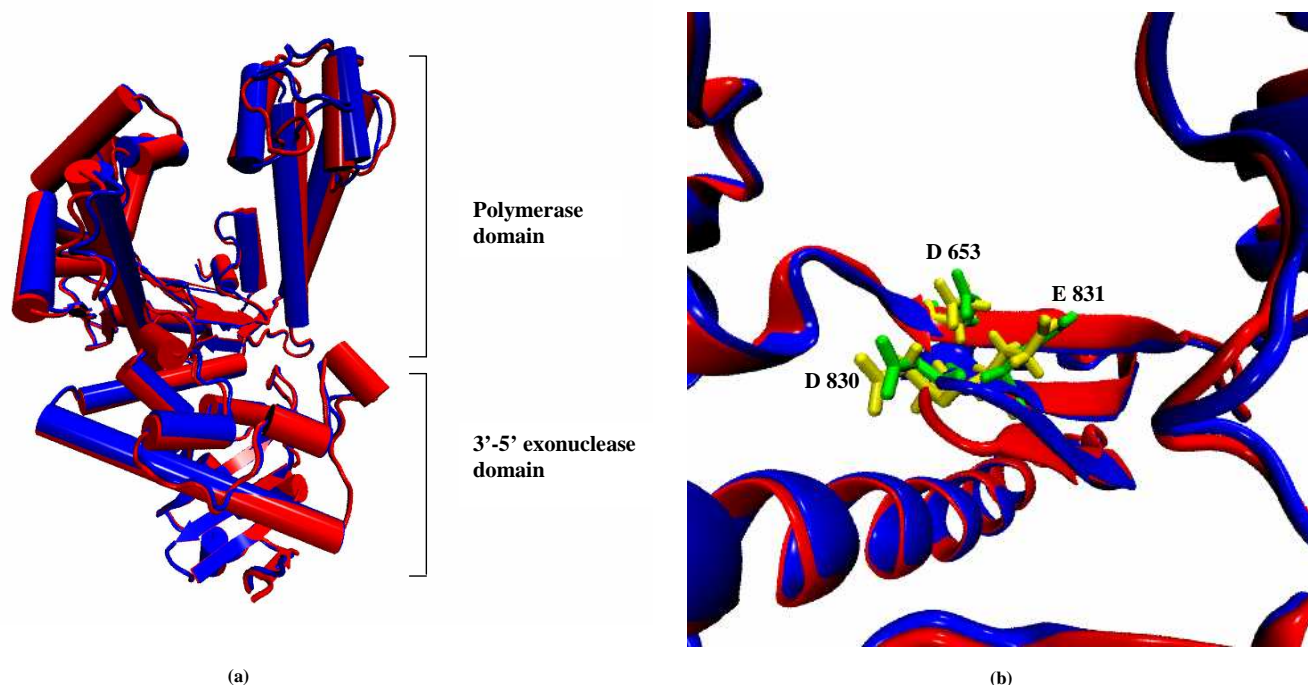


Fig. (1). (a) Fitting of the backbone atoms of BF from *B. stearotermophilus* (1XWL) (blue) and the corresponding of DNA Pol I ITB-1 (red). The proteins were shown as cartoon. (b) Stereodiagram of polymerase active site of BF from *B. stearotermophilus* (blue) and DNA Pol I ITB-1 (red). Three conserved carboxylate residues (triad carboxylate) which were essential for catalysis in active site of BF and DNA Pol I ITB-1 were shown in green and yellow licorice form (Drawn with VMD 1.8.6).

structure of its template with the RMSD value 1.46 Å (Fig. 1a). All structural features in the polymerase domain, such as palm, thumb, and fingers were similar to those found in known DNA Pol I structure. In addition, the orientation and geometry of residues involved in the active site of the polymerase domain e.g. Asp 653, Asp830 and Glu831 [45], were similar to those found in BF polymerase domain, illustrated in Fig. (1b). In addition, the exonuclease domain also exhibited similar conformational feature with the editing domain of BF. All these structural features indicated that the structural model of DNA Pol I ITB-1 was successfully determined and reliable to be used as an initial coordinate for molecular dynamic simulation in this study.

Conformational Dynamics of DNA Pol I ITB-1

MD simulations of DNA Pol I ITB-1 were carried out at temperature 300K and 350K in implicit solvent, using the generalized Born solvation model [46]. The simulation at 300K was intended to assess the conformational stability of DNA Pol I ITB-1 at room temperature. Meanwhile, the simulation at 350K was performed to elucidate the early stage of unfolding and investigated factors that have important role in maintaining thermal stability of the protein. The simulations covered root-mean-square deviation (RMSD), root-mean-square fluctuation (RMSF), solvent accessible surface area (SASA), and percentage of secondary structure (%SS) analyses.

The RMSD represented the structural changes during the simulation [47, 48]. Analysis for the time evolution-RMSD resulted from the simulation at 300K and revealed that the structure was fluctuated at around 4 to 6 Å from the initial structure, as shown in Fig. (2a). Alignment between the

structure after 1 ns with the initial (0 ns), showed that the average RMSD difference was about 5 Å. The stability of the protein structure at room temperature justified the reliability of the implicit solvent system used in this study. In contrast, the simulation at 350K exhibited different C α RMSD profile. Initially, the RMSD value remained almost constant at around 9 Å until ~ 0.60 ns, and then sharply increased up to ~29 Å at about 0.89 ns and then fluctuated at around the value. The amplitude during the fluctuation after the transition had increased tendency and reached to 35 Å at about 2 ns (Fig. 2a). The appearance of sharp transition of RMSD within 0.60-0.89 ns indicated that there was cooperative unfolding event at 350K simulation. The existence of the transition indicated that temperature at 350K was suitable to study the early unfolding step of DNA Pol I ITB-1.

Further analysis on the flexibility profile of individual amino acid residues in the enzyme at 350K were calculated by root mean square fluctuation (RMSF), as a function of residue number. RMSF analysis at 350K showed that there were several extreme values exhibited by amino acid residues in certain positions as indicated by the appearance of some peaks in the RMSF plot (Fig. 2b). The position of residues corresponded to the peaks was located in both 3'→5' exonuclease and 5'→3' polymerase domains. The residues within 3'→5' exonuclease domains were located at the position of 326, 425-427 and 430-433, whereas the residues in the polymerase domain were located at the positions of 521-524 and 550-552. In order to clarify the locations of the flexible regions in the structure of DNA Pol I ITB-1, the RMSF value of individual residues was converted into β -factors [49-50] and then the result was mapped into the structure of protein, as shown in Fig. (2c).

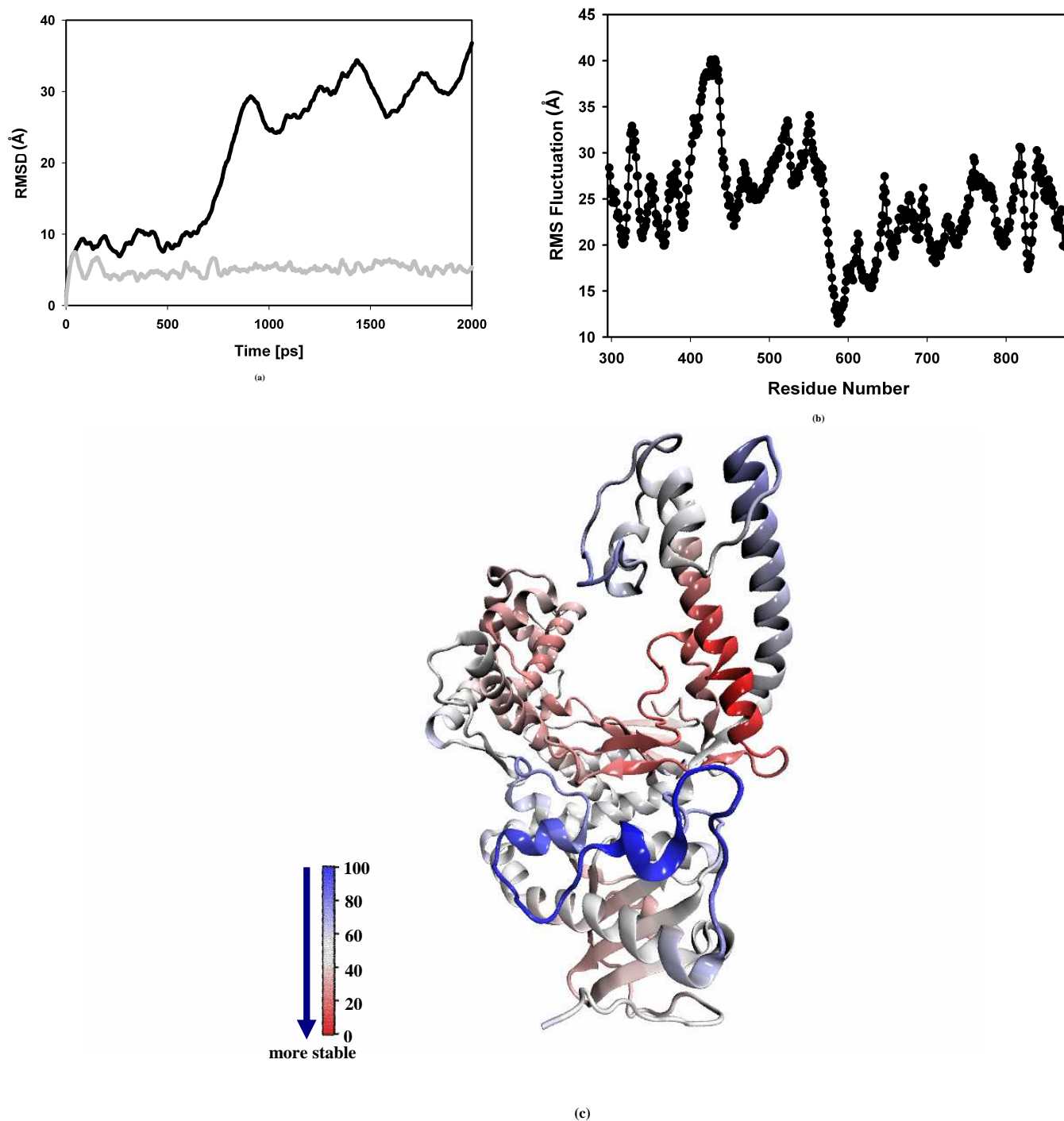


Fig. (2). (a) RMSD (Å) of the backbone atoms for DNA Pol I ITB-1 at 300K (grey) and at 350K (black). (b) Shows the RMSF as a function of residue number at 350K. (c) Thermostability map of DNA Pol I ITB-1 based on β -factor value of the unfolding simulation at 350 K.

The β -factor value of individual residue was distinguished in the map by RGB (Red Green Blue) color scale, where the lowest to highest values were showed as gradation color from red to blue. As shown from the map, it was found that the rigid as well as flexible regions were not concentrated in a particular region, but distributed in the two domains of DNA Pol I ITB-1. Nevertheless, the numbers of flexible segments were relatively higher in the 3'→5' exonuclease as compared to those in the 5'→3' polymerase domain. This indicated that the former domain was more sensitive to heat.

Previous study at higher temperatures (400K and 500K) also revealed that the 3'→5' exonuclease domain had lower thermostability as compared to that of polymerase domain [35].

In order to investigate detailed conformational changes, solvent accessible surface area (SASA) was calculated especially for the whole surface area and non-polar region as a function of time. Similar to RMSD profile, it was also observed that there was a transition in the total SASA value

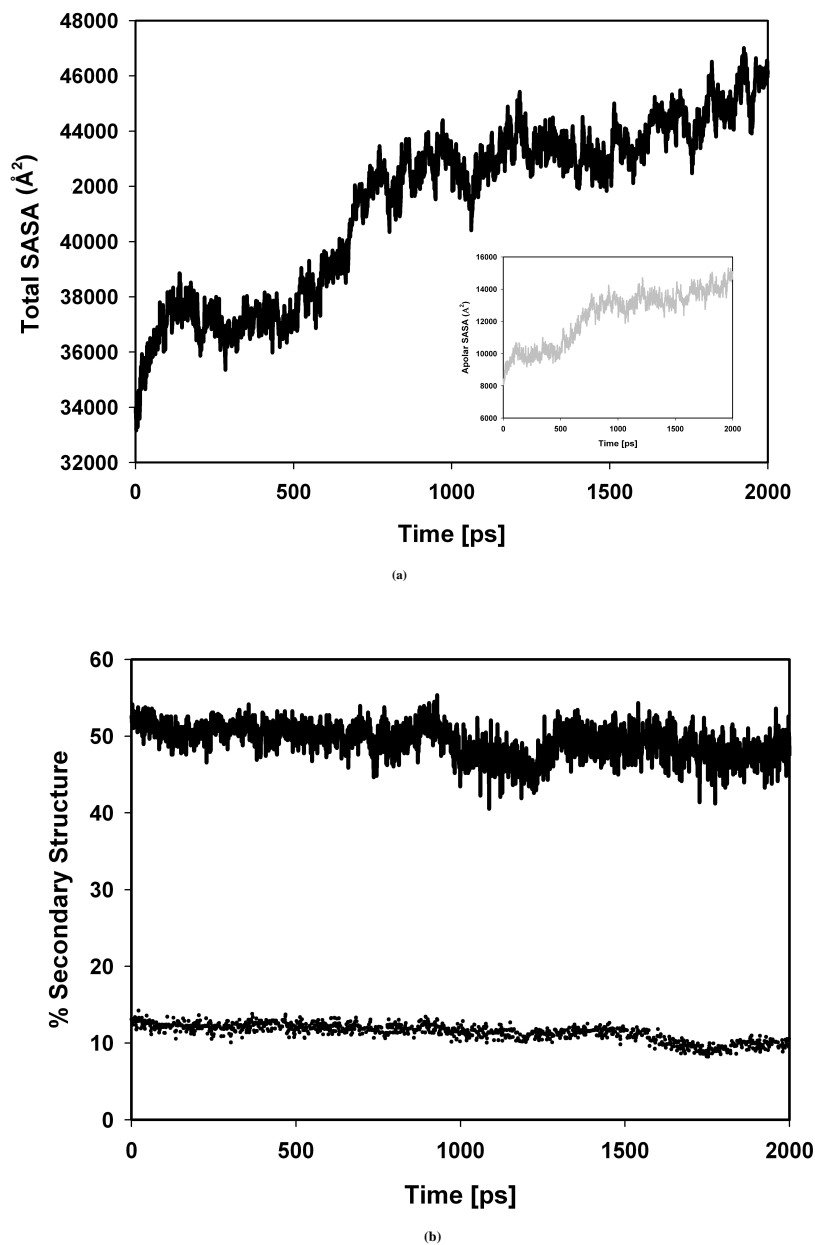


Fig. (3). (a) Total SASA values (solid line) and apolar SASA values for 350K simulation in insert picture (b) Percentage of secondary structure for the DNA pol I ITB-1 during 350 K simulation, α helix (solid line) and β sheet (dots).

at similar time range e.g. between 0.6 and 0.9 ns, thereby the two observations were in agreement with each others (Fig. 3a). Calculation for time evolution of non-polar SASA further clarified the observed profile of total SASA and RMSD values. The transition within the same time range was also found in non-polar SASA. All these suggested that within this time range the non-polar residues buried in the interior of the protein were suddenly exposed to the solvent. (Fig. 3a, insert).

Besides the investigation of the global conformational change at tertiary structure, the secondary structure was also evaluated. In contrast to the profile found in RMSD and SASA, the secondary structure content for both α -helices and β -sheets decreased gradually by the simulation time (Fig. 3b) without any sudden apparent transition. The data suggested

that the conformational change during MD simulation at 350K mostly affected the tertiary structure of the protein rather than its secondary structures.

Early Unfolding Event of DNA Pol I ITB-1

The unfolding profile of DNA Pol I ITB-1 was followed by analysis of the trajectories profiles. The results showed that the interface of the two domains were suddenly separated, exposing the buried amino acid residues on the solvent. It was also noticed that such event did not immediately trigger the unfolding of the individual domain (Fig. 4). The interactions within the interface were not the factor that not only determine the stability of individual domains but also the overall structure of the protein. The residues within the interface domain were apparently more

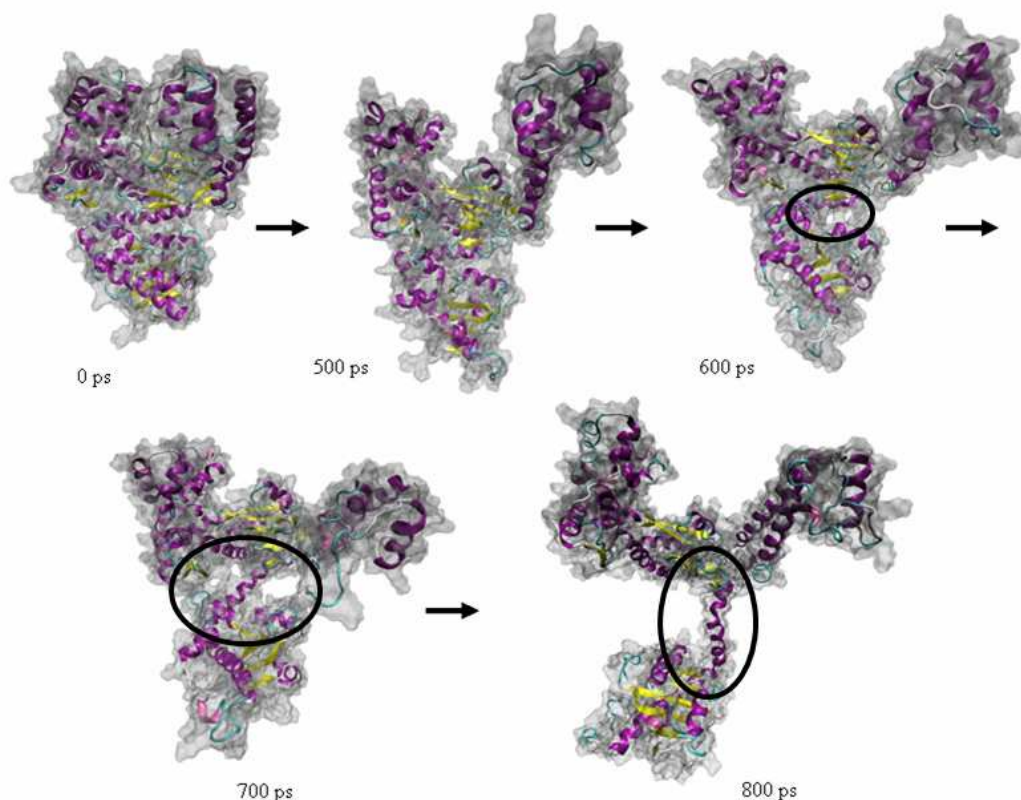


Fig. (4). The conformational changes of DNA Pol I ITB-1 observed in the unfolding trajectory at 350K simulation. The circles indicating the early events in unfolding process. (Drawn with VMD 1.8.6).

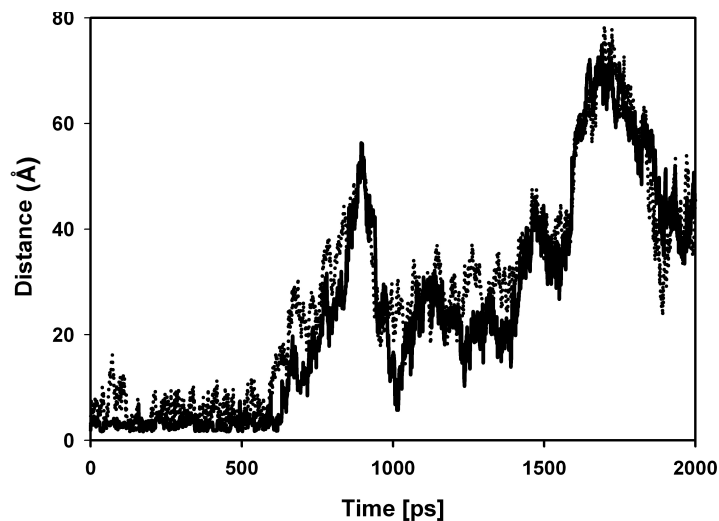


Fig. (5). The distance of Lys374-Glu489 (solid line) and Lys381-Glu487 (dash line) during the 350K simulation.

affected by thermal perturbation at 350K as compared to the residues within the individual domains of the protein.

In order to identify amino acids residues responsible for the stability in the interface domain, further analysis was carried out focusing on the separation of the two domains. It was found that at least two pairs of amino acid residues, Lys374-Glu489 and Lys381-Glu487, were apparently responsible for the stability of the interface domain. The two pairs formed salt bridges at the interface between 5'→3' polymerase and 3'→5' exonuclease domains of DNA Pol I

ITB-1. The distance of these interactions during simulation was shown in Fig. (5). The results showed that the salt bridges formed by pairs of Lys374-Glu489 and Lys381-Glu487 were initially stable until the simulation was running up to 0.6 ns. However, between 0.6 to 0.9 ns, the interactions were cooperatively broken as indicated by the sudden increase of the pair distances. These events were occurred at the same time with those found in RMSD and SASA (Fig. 2a, 3a). The data suggested that intermolecular interactions within the two pairs of residues, Lys374-Glu489 and

Lys381-Glu487, played important role in maintaining the interface contact between 5'→3' polymerase and 3'→5' exonuclease domains.

After domain separation, it was shown that the individual domain, 5'→3' polymerase and 3'→5' exonuclease domains, remained in the folded state. This condition was persisted until the simulation time reached at 2 ns, then each of the domain was gradually unfolded. Therefore, the unfolding of DNA Pol I ITB-1 was occurred sequentially and the domain separation was the early event of the unfolding.

Effect of Mutation at the Interface Domain on Thermal Stability of the Enzyme

In order to further identify the role of the ionic interaction in the interface domain, four hypothetic mutants were constructed by substituting one of the amino acid residues in each pairs, namely Glu487Gln, Glu489Gln, Glu487Asp, Glu489Asp. The first two mutants (Glu487Gln and Glu489Gln) were designed to change the electrostatic interaction into charge-neutral hydrogen bond between the side chains. The last two mutants, Glu487Asp and Glu489Asp, were constructed to improve the electrostatic interaction at the site. The effects of the mutation were evaluated by calculating solvation free energy changes ($\Delta\Delta G_{\text{solv}}$) using FEP method.

Replacements of Glu487 to Gln showed positive value of $\Delta\Delta G_{\text{solv}}$ e.g. + 53.67 kcal/mol, indicating that the protein become unstable as compared to that the wildtype (Fig. 6). In addition, the calculation of $\Delta\Delta G_{\text{solv}}$ for mutant Glu489Gln also showed positive value of $\Delta\Delta G_{\text{solv}}$ (data not shown). In contrast, the mutation of Glu487Asp and Glu489Asp reduced $\Delta\Delta G_{\text{solv}}$ up to, -21.5 and -14.1 kcal/mol, respectively (Fig. 6).

DISCUSSION

MD simulations were carried out at temperature 300K and 350K in implicit water, using the generalized Born

solvation model [46]. The advantage of using the implicit water system is significant reduction of the number of atoms involved in the calculations, thereby the calculations becoming faster [38]. Many reports showed comparable result of the implicit water system in their study relative to those obtained by using the explicit solvent [51-54]. The reliability of the solvent system was evaluated in our study by taking the simulation result at 300K as reference. The stability of protein exhibited in the simulation at this temperature proved the reliability of the solvent system. Caflisch and coworkers [55] have pioneered long folding simulations using simple peptide, the α -helical (AAQAA)₃ and the β -hairpin-forming sequence V₅DPGV₅ by implicit solvent models. By using low (or no) viscosity in the simulations, the study could speed up the timescales occupied in folding. Additional benefit of using implicit solvent is the time for conformational samples that are obtained in relatively shorter time period. The advantages enabled to focus the analysis on intra-molecular interactions within the protein [56], as in the current study to locate key residues in DNA Pol I ITB-1, whose interactions are important for protecting the structure from thermal perturbation. The analysis will be obscured by intermolecular contact with water molecules, since it is complicated to discriminate molecular events occurred due to conformational dynamics imposed by intra-molecular interaction within the protein or due to intermolecular contact with water molecule [38].

MD simulation at 300K were also used to assess the reliability of the structural model of DNA Pol I ITB-1, obtained from the comparative modeling program. Simulation at 300K revealed the typical conformational motion of DNA Pol I, which are periodically open and closed motions of the polymerase domain. As reported in the previous work, such motions are important for their enzymatic activity during the polymerization process of DNA [36, 57-58]. The similarity in conformational motion of DNA Pol I ITB-1 with the other DNA Pol I proved the reliability of the structural model used in this study.

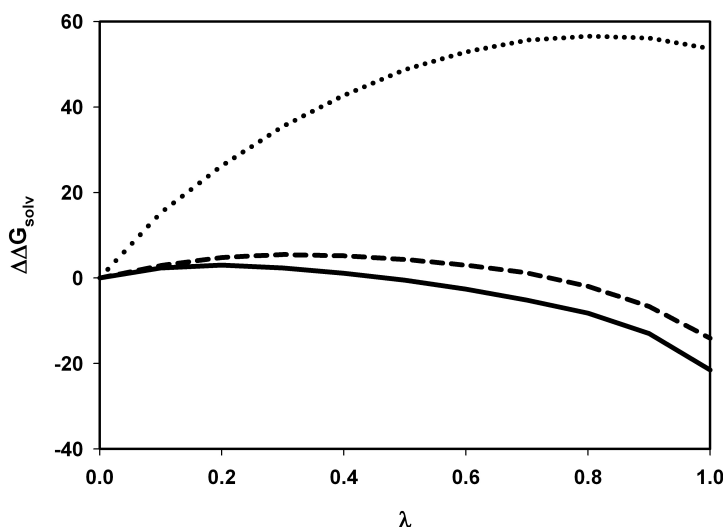


Fig. (6). The curve of solvation free energy changes as a function of coupling parameter (λ) for three mutants: Glu487Asp (solid line), Glu487Gln (dots) and Glu489Asp (dash line).

Previous studies showed that DNA Pol I ITB-1 has optimum polymerase temperature at 338K [34]. Hence, to observe the unfolding profile and factors that determined the stability of the protein, we presented the 350K simulations, above its optimum temperature. Day *et al.* [28] have shown that by increasing temperature, unfolding of chymotrypsin inhibitor 2 (CI2) was accelerated, without altering the pathway of unfolding. Meanwhile, Li and Dagget [27] used high-temperature MD simulation of CI2 to speed up the kinetic unfolding of protein. This method was based on the assumption that most of the thermal unfolding of protein has Arrhenius behavior, and therefore, the increasing temperature does not change the unfolding pathway of protein [59]. Thermal unfolding simulation at 350K revealed that DNA Pol I ITB-1 unfolded sequentially. It has been shown that the unfolding was initiated by the domain separation between 5'→3' polymerase and 3'→5' exonuclease domains. It has also been shown that there are two salt-bridges (Lys374-Glu489 and Lys381-Glu487) buried in the hydrophobic interface between 5'→3' polymerase and 3'→5' exonuclease domains, taking role in tightening the contact of the two domains. As long as the two salt-bridges existed, the protein molecules still showed normal structure and functions as we noted in the existence of open and closed conformational motions for about 0.6 ns. After the domain separation occurred, however, such conformational motion was disrupted. It was also noted that, this event was not spontaneously followed by the unfolding of individual domains. The 5'→3' polymerase and 3'→5' exonuclease domains were still in the folded structure until the simulation time reached at 2 ns (Fig. 2a). This implies that interface contacts between 5'→3' polymerase and 3'→5' exonuclease domains are most likely the transition state to reach the native conformation in the folding mechanism of DNA Pol I ITB-1. The two salt-bridges are also directing the proper contact between the two domains besides tightening the contact between them, since these interactions are the only specific interactions at the interface domain.

In this study, four mutations were constructed *in silico* to change the stability of the interface domain, namely Glu487Gln, Glu489Gln, Glu487Asp, and Glu489Asp. The first two mutants were designed to disrupt the ionic interaction, while the last two mutants were designed to tighten the ionic interaction. Based on the free-energy calculations, only mutations of Glu487Asp and Glu489Asp were increased the thermal stability of the enzymes. Similar observation has recently been reported with a *Flavobacterium meningosepticum* glycerol kinase [23]. Thermal stability of glycerol kinase was enhanced by improving the electrostatic interaction in the interface region. Exclusively, the work of Waksman and colleagues on Klenow-like *Thermus aquaticus* DNA Pol I (Klentaq1) demonstrated that the ionic interaction at the interface domain also contributes for thermal stability of the protein [60]. A number of studies also suggested that increasing or enhancing electrostatic interaction in thermophilic and mesophilic proteins were used to increase thermal stability of proteins [61-64]. Theoretical models by Elcock [65] showed that electrostatic interaction could make a positive contribution to protein stability at high temperature. Based on Elcock postulates, there was a significant energetic barrier for breaking a salt bridge in the protein.

All the data showed that the electrostatic interaction at the interface domain might be responsible for the stability of the enzyme, because change of the electrostatic interaction into charge-neutral hydrogen bond (Glu487Gln and Glu489Gln) decreased the thermal stability of the DNA Pol I ITB-1. Moreover, improvement in the electrostatic interaction (Glu487Asp and Glu489Asp) stabilized the tertiary structure of DNA Pol I ITB-1.

CONCLUSION

MD simulation of DNA Pol I ITB-1 at 350K provided information on dynamic characteristics, especially on domain flexibility and early unfolding process. The results showed that thermo-labile and thermo-stable regions were dispersed through out the protein. However, the amounts of thermo-labile regions were higher in the 3'→5' exonuclease domain as compared to that of the polymerase domain. The simulations also provided the early unfolding process of DNA Pol I ITB-1. This process was caused by domain separation which was triggered by the broken electrostatic interactions between Lys381-Glu487 and Lys374-Glu489. The free-energy perturbation showed that the substitution of Glu487 by Gln, and Glu489 by Gln decreased the stability of enzyme. Meanwhile, replacement of Glu to Asp at position 487 and 489 enhanced the electrostatic interaction at the interface domain, and thus, stabilizing the enzyme. All the data suggested that the salt bridges were responsible for stability of the interface domain of DNA Pol I ITB-1.

ACKNOWLEDGEMENTS

We are grateful for partially financial support from Institut Teknologi Bandung (ITB Research Grant No 0004/K01.03.2/PL2.1.5/I/2006 and No.174/K01 07/PL/2007) and State Ministry of Research and Technology (06/RD/Insentif/PPK/II/2008) to RH and ITB scholarship (voucher) to SN.

CONFLICT OF INTEREST

The authors have declared that no conflict of interest exists.

REFERENCES

- [1] Delarue M, Poch O, Tordo N, Moras D, Argos P. An attempt to unify the structure of polymerases. *Protein Eng* 1990; 3(6): 461-7.
- [2] Braithwaite DK, Ito J. Compilation, alignment and phylogenetic relationships of DNA polymerase. *Nucl Acids Res* 1999; 21: 787-802.
- [3] Joyce CM, Steitz TA. Function and structure relationships in DNA polymerases. *Annu Rev Biochem* 1994; 63: 773-822.
- [4] Patel PH, Loeb LA. DNA polymerase active site is highly mutable: Evolutionary consequences. *Proc Natl Acad Sci USA* 2000; 97: 5095-100.
- [5] Konberg A. Minireview: DNA replication. *J Biol Chem* 1988; 236: 1-4.
- [6] Steitz T. DNA polymerase: structural diversity and common mechanisms. *J Biol Chem* 1999; 274: 17395-8.
- [7] Brautigam CA, Steitz TA. Structural and functional insights provided by crystal structures of DNA polymerases and their substrate complexes. *Curr Opin Struct Biol* 1998; 8: 54-63.
- [8] Mullis K, Falooma F, Saiki R, Horn G, Erlich H. Specific enzymatic amplification of DNA *in vitro*: the polymerase chain reaction. *Cold Spring Harb Symp Quant Biol* 1986; 247: 7116-22.
- [9] Saiki RK, Gelfand DH, Stoffel S, Scharf S, Higuchi R, Horn GT, Mullis KB, Erlich HA. Primer-directed enzymatic amplification of

- DNA with a thermostable DNA polymerase. *Science* 1998; 239: 487-91.
- [10] Blöndal T, Sigridur TH, Kieleczawa J, Hjörleifsdóttir S, Kristjánsson JK, Einarsson JM, Eggertsson G. Cloning, sequence analysis and functional characterization of DNA polymerase I from the thermophilic eubacterium *Rhodothermus marinus*. *Biotechnol Appl Biochem* 2001; 34: 37-45.
- [11] Choi JJ, Jung SE, Kim H, Kwon S. Purification and properties of *Thermus filiformis* DNA polymerase expressed in *Escherichia coli*. *Biotechnol Appl Biochem* 1999; 30: 19-25.
- [12] Kim BC, Grote R, Lee DW, Antranikian G, Pyun YR. *Thermoanaerobacter yonseiensis* sp. a novel extremely thermophilic, xylose-utilizing bacterium that grows at up to 85°C. *Int J Sys Evol Microbiol* 2001; 51: 1539-48.
- [13] Shin HJ, Lee SK, Choi JJ, Koh S, Lee JH, Kim SJ, Kwon ST. Cloning, expression and characterization of a family B-type DNA polymerase from the hyperthermophilic crenarchaeon *Pyrobaculum arsenaticum* and its application to PCR. *J Microbiol Biotechnol* 2005; 15: 1359-67.
- [14] Kim YJ, Lee HS, Bae SS, Jeon JH, Lim JK, Cho Y, Nam KH, Kang SG, Kim SJ, Kwon ST, Lee JH. Cloning, purification and characterization of a new DNA polymerase from a hyperthermophilic archaeon *Thermococcus* sp. NA1. *J Microbiol Biotechnol* 2007; 17: 1090-7.
- [15] Akhmaloka, Tika IN, Nurbaiti S, Sindumarta M, Madayanti F. Isolation and characterization of a novel thermostable DNA polymerase from *Bacillus thermophilus* sp1. *Indonesian J Microbiol* 2006; 11(2): 82-6.
- [16] Perler FB, Kumar S, Kong H. Thermostable DNA polymerases. *Adv Prot Chem* 1996; 48: 377-435.
- [17] Stenesh J, Roe RA. DNA polymerase from mesophilic and thermophilic bacteria. Purification and properties of DNA polymerase from *Bacillus licheniformis* and *Bacillus stearothermophilus*. *Biochem Biophys Acta* 1972; 272: 156-66.
- [18] Kaboev OK, Luchkina LK, Akhmedov AT, Bekker ML. Purification and properties of deoxynucleic acid polymerase from *Bacillus stearothermophilus*. *J Bacteriol* 1981; 145(1): 21-6.
- [19] Sellman E, Schroder KL, Knoblich IM, Westermann P. Purification and characterization of DNA polymerase from *Bacillus* species. *J Bacteriol* 1992; 174: 4350-5.
- [20] Uemori T, Ishino Y, Fujita K, Asada K, Kato I. Cloning of the DNA polymerase gene of *Bacillus caldotenax* and characterization of the gene product. *J Biochem* 1993; 113: 401-10.
- [21] Vieille C, Zeikus GJ. Hyperthermophilic enzymes: sources, uses, and molecular mechanisms for thermostability. *Microbiol Mol Biol Rev* 2001; 65(1): 1-43.
- [22] Luisi DL, Snow CD, Lin JJ, Hendsch ZS, Tidor B, Raleigh DP. Surface salt bridges, double-mutant cycles, and protein stability: an experimental and computational analysis of the interaction of the Asp 23 side chains with the N-terminus of the N-terminal domain of the ribosomal protein L9. *Biochemistry* 2003; 42: 7050-60.
- [23] Sakasegawa S, Takehara H, Yoshioka I, Takahashi M, Kagimoto Y, Misaki H, Sakuraba H, Ohshima T. Increasing the thermostability of *Flavobacterium meningosepticum* glycerol kinase by changing Ser329 to Asp in the subunit interface region. *Protein Eng* 2001; 14(9): 663-7.
- [24] Lu HL, Wang WC. Protein engineering to improve the thermostability of glucoamylase from *Aspergillus awamori* based on molecular dynamics simulations. *Protein Eng* 2003; 16: 19-25.
- [25] Farias ST, Bonato MCM. Preferred amino acids and thermostability. *Gen Mol Res* 2003; 2(4): 383-93.
- [26] Hanson T, Oostenbrink C, van Gunsteren WF. Molecular dynamics simulations. *Curr Opin Struc Biol* 2002; 2: 190-6.
- [27] Li A, Dagget V. Characterization of the transition state of protein unfolding by use of molecular dynamics : chymotrypsin inhibitor 2. *Proc Natl Acad Sci USA* 1994; 91: 10430-4.
- [28] Day R, Bennion BJ, Ham S, Daggett V. Increasing temperature accelerates protein unfolding without changing the pathway of unfolding. *J Mol Biol* 2002; 322: 189-203.
- [29] Levitt M, Sharon R. Accurate simulation of protein dynamics in solution. *Proc Natl Acad Sci USA* 1988; 85: 7557-61.
- [30] Lu B, Wong CF, McCammon JA. Release of ADP from the catalytic subunit of protein kinase A: a molecular dynamics simulation study. *Protein Sci* 2005; 14: 159-68.
- [31] Hoppe C, Schomburg D. Prediction of protein thermostability with a direction- and distance-dependent knowledge-based potential. *Protein Sci* 2005; 14: 2682-92.
- [32] Tsaia J, Levitt M. Evidence of turn and salt bridge contributions to b-hairpin stability: MD simulations of C-terminal fragment from the B1 domain of protein G. *Biophys Chem* 2002; 101-102: 187-201.
- [33] Sham YY, Ma B, Jung TC, Nussinov R. Thermal unfolding molecular dynamics simulation of *Escherichia coli* dihydrofolate reductase: thermal stability of protein domains and unfolding pathway. *Proteins* 2002; 46(3): 308-20.
- [34] Akhmaloka, Pramono H, Ambarsari L, Susanti E, Nurbaiti S, Madayanti F. Cloning, homological analysis, and expression of DNA Pol I from *Geobacillus thermoleovorans*. *IJIB* 2007; 1(3): 206-15.
- [35] Hertadi R, Nurbaiti S, Akhmaloka. Molecular dynamics analysis of thermostable DNA Pol I ITB-1. *Microbiol Indonesia* 2007; 1(3): 101-4.
- [36] Beese LS, Derbyshire V, Steitz TA. Structure of DNA polymerase I Klenow Fragment bound to duplex DNA. *Science* 1993; 260: 352-5.
- [37] Rost B, Yachdav G, Liu J. The predict protein server. *Nucl Acids Res* 2004; 32: W321-6.
- [38] Case DA, Cheatham TE III, Darden T, Gohlke H, Luo R, Merz KM, Onufriev A, Simmerling C, Wang B, Woods RJ. The Amber biomolecular simulation programs. *J Comput Chem* 2005; 26: 1668-88.
- [39] Raykaert JP, Ciccotti G, Berendsen HJC. Numerical integration of the cartesian equations of motion of a system with constraints : molecular dynamics of n-Alkenes. *J Comput Phys* 1977; 23: 327-41.
- [40] Duan Y, Wu C, Chowdhury S, Lee MC, Xiong G, Zhang W, Yang R, Cieplak P, Luo R, Lee T, Caldwell J, Wang J, Kollman P. A point-charge force field for molecular mechanics simulations of proteins. *J Comput Chem* 2003; 24: 1999-2012.
- [41] Humphrey W, Dalke A, Schulten K. VMD-Visual Molecular Dynamics. *J Molec Graphics* 1996; 14: 33-8.
- [42] James CP, Braun R, Wang W, Gumbart J, Tajkhorshid E, Villa E, Chipot C, Skeel RD, Kalé L, Schulten K. Scalable molecular dynamics with NAMD. *J Comput Chem* 2005; 26: 1781-802.
- [43] Kabsch W, Sander C. Dictionary of protein secondary structure: pattern recognition of hydrogen-bonded and geometrical features. *Bio polymers* 1983; 2(12): 2577-637.
- [44] Kiefer JR, Mao C, Hansen CJ, Basehore SL, Hogrefe HH, Braman JC, Beese LS. Crystal structure of a thermostable *Bacillus* DNA polymerase I large fragments at 2.1 Å resolution. *Structure* 1997; 5: 95-108.
- [45] Polesky AH, Steitz TA, Grindley NDF, Joyce CM. Identification of residues critical for the polymerase activity of the Klenow Fragment of DNA polymerase I of *Escherichia coli*. *J Biol Chem* 1990; 265: 14579-91.
- [46] Onufriev A, Bashford D, Case DA. Exploring protein native states and large-scale conformational changes with a modified generalized Born model. *Proteins* 2004; 55: 383-94.
- [47] Becker OM, MacKerell Jr AD, Roux B, Watanabe M, Eds. *Computational Biochemistry and Biophysics*. New York: Marcel Dekker; 2001.
- [48] Coutsiar EA, Seok C, Dill KA. Using quaternions to calculate RMSD. *J Comput Chem* 2004; 25: 1849-57.
- [49] van Gunsteren WF, Mark AE. Validation of molecular dynamics simulation. *J Chem Phys* 1998; 108: 6109-16.
- [50] Voordijk S, Hansson T, Hilvert D, van Gunsteren WF. Molecular dynamics simulations highlight mobile regions in proteins: a novel suggestion for converting a murine V_H domain into a more tractable species. *J Mol Biol* 2000; 300(4): 963-73.
- [51] Shen M, Freed KF. Long time dynamics of met-enkephalin: comparison of explicit and implicit solvent models. *Biophys J* 2002; 82: 1791-808.
- [52] Lin JH, Baker NA, McCammon JA. Bridging implicit and explicit solvent approaches for membrane electrostatics. *Biophys J* 2002; 83: 1374-9.
- [53] Huang A, Stultz CM. Conformational sampling with implicit solvent models: application to the PHF6 peptide in Tau protein. *Biophys J* 2007; 92: 34-45.
- [54] Freddolino PL, Liu F, Grubbe M, Schulten K. Ten-microsecond MD simulation of a fast-folding WW domain. *Biophys J* 2008; 94: L75-7.

- [55] Ferrara P, Apostolakis J, Caflisch A. Thermodynamics and kinetics of folding of two model peptides investigated by molecular dynamics simulations. *J Phys Chem* 2000; B104: 5000-10.
- [56] Sekijima M, Motono C, Yamasaki S, Kaneko K, Akiyama Y. Molecular dynamics simulation of dimeric and monomeric forms of human prion protein: insight into dynamics and properties. *Biophys J* 2003; 85: 1176-85.
- [57] Li Y, Korolev S, Waksman G. Crystal structures of open and closed forms of binary and ternary complexes of the large fragment of *Thermus aquaticus* DNA polymerase I: structural basis for nucleotide incorporation. *EMBO J* 1998; 17: 7514-25.
- [58] Kiefer J, Mao C, Braman J, Beese L. Visualizing DNA replication in a catalytically active *Bacillus* DNA polymerase crystal. *Nature* 1998; 391: 304-7.
- [59] Wang T, Wade RC. On the use of elevated temperature in simulations to study protein unfolding mechanisms. *J Chem Theory Comput* 2007; 3: 1476-83.
- [60] Korolev S, Nayal M, Barnes WM, di Cera E, Waksman G. Crystal structure of the large fragment of *Thermus aquaticus* DNA polymerase I at 2.5-Å resolution: Structural basis for thermostability. *Proc Natl Acad Sci USA* 1995; 92: 9264-8.
- [61] Aguilar CF, Cronin NB, Badasso M, Dreyer T, Newman MP, Cooper JB, Hoover DJ, Wood SP, Johnson MS, Blundell TL. The three dimensional structure at 2.4 Å resolution of glycosylated proteinase A from the lysosome-like vacuole of *Saccharomyces cerevisiae*. *J Mol Biol* 1997; 257: 899-915.
- [62] Xiao L, Honig B. Electrostatic contributions to the stability of hyperthermophilic protein. *J Mol Biol* 1999; 289: 1435-44.
- [63] Kumar S, Ma YB, Tsai CJ, Nussinov R. Electrostatic strengths of salt bridges in thermophilic and mesophilic glutamate dehydrogenase monomers. *Proteins: Struct Funct Genet* 2000; 38: 368-83.
- [64] Vogt G, Woell S, Argos P. Protein thermal stability, hydrogen bonds, and ion pairs. *J Mol Biol* 1997; 269: 631-43.
- [65] Elcock AH. The stability of salt bridges at high temperatures: implications for hyperthermophilic proteins. *J Mol Biol* 1998; 284: 489-502.

Received: October 08, 2008

Revised: November 24, 2008

Accepted: December 29, 2008

© Nurbaiti *et al.*; Licensee Bentham Open.

This is an open access article licensed under the terms of the Creative Commons Attribution Non-Commercial License (<http://creativecommons.org/licenses/by-nc/3.0/>), which permits unrestricted, non-commercial use, distribution and reproduction in any medium, provided the work is properly cited.